

## Relativistic Corrections in the Theory of $K$ -Electron Ejection During $K$ Capture

R. L. INTEMANN

*Department of Physics, Temple University, Philadelphia, Pennsylvania 19122*

(Received 19 August 1968)

The momentum spectrum of the  $K$  electrons ejected during allowed  $K$ -capture decay is calculated for the case in which there is no competing positron emission. It is shown that certain relativistic effects, associated with the spin of the electron, are important in determining the ejected-electron spectrum, even at low energies. To take these effects into account, the electronic states are described by the solutions of an approximate Dirac Hamiltonian developed by Biedenharn and Swamy. Preliminary to the calculation, both the eigenfunctions and Green's function of this Hamiltonian are discussed. The results of the calculation differ appreciably from previous nonrelativistic calculations. Contrary to these previous theories, the theory presented here is shown to be in good agreement with recent experimental observations.

### I. INTRODUCTION

IT is well known that during orbital electron capture, there is present a continuous spectrum of ejected orbital electrons.<sup>1</sup> The intensity of this electron spectrum was first calculated by Primakoff and Porter.<sup>2</sup> Their treatment of the problem is a nonrelativistic one (with the exception of the description of the neutrino) and is based on the use of the sudden perturbation approximation. In their approach, the initial two-electron state is described by a two-parameter variational wave function, designed to take account of screening and correlation effects and adjusted to minimize the energy of the initial electronic configuration.<sup>3</sup>

Since the development of the Primakoff-Porter theory, the ejected-electron spectrum has been measured in four cases<sup>4-7</sup>; however, only the Daniel-Schupp-Jensen study<sup>6</sup> of  $\text{Cs}^{131}$  and the Pengra-Crasemann study<sup>7</sup> of  $\text{Fe}^{55}$  have covered a substantial energy range. In all cases a pronounced discrepancy has been observed at low energies, the experimentally measured intensities being lower than those predicted by the Primakoff-Porter theory.

In an attempt to resolve these discrepancies, we<sup>8</sup> have recently developed a new theory in which the initial-state electron-electron interaction is treated as a perturbation along with the  $\beta$  interaction. Because the discrepancies are so large (as much as a factor of 5 in the spectrum of  $\text{Fe}^{55}$ ) and occur at low electron energies ( $\lesssim 50$  keV for  $\text{Fe}^{55}$ ), it was felt that a nonrelativistic treatment of the electronic motions would be sufficient to bring theory and experiment into much better agree-

ment. Consequently, the appropriate nonrelativistic Coulomb wave functions and Coulomb Green's function were employed in the description of the various electron states. The ejected-electron spectrum resulting from this theory turned out to be virtually identical with that predicted by the Primakoff-Porter theory for almost the entire energy range of the ejected electrons—a rather surprising result.

As has already been pointed out in I, the greatest source of error in both the Primakoff-Porter theory and the theory of I is the neglect of relativistic effects. However, contrary to our conclusions in I, relativistic corrections are indeed large, as may be made plausible by an argument originally advanced by Martin and Glauber<sup>9</sup> in connection with their discussion of radiative  $K$  capture. Their argument is equally applicable here and simply emphasizes the fact that the electron ejection process must always involve the essentially relativistic electron spin. This is because, for an allowed transition<sup>10</sup> to occur from the  $K$  shell, the electron undergoing capture is required to emit a photon during a transition from one spherically symmetric state to another. This cannot be done by a spinless particle; hence the spin enters in an essential way.

In fact, the inclusion of relativistic effects will tend to alter the shape of the theoretical spectrum in such a way as to bring it into closer agreement with the experimental data. That this is so is most easily seen from the Primakoff-Porter theory. In this theory the matrix element for the ejection process is essentially an overlap integral between the initial and final states of the ejected electron. For the purpose of the present argument we may assume the initial-state wave function to be simply a  $1s$  nonrelativistic hydrogenic wave function. The screening and correlation factors may be ignored since, as the Primakoff-Porter calculation shows, their only effect is to change the atomic number of the parent nucleus very slightly and to introduce an over-all multiplicative constant into the matrix element. However, they have essentially no influence on

<sup>1</sup> For a review of recent results, see D. Berényi, *Rev. Mod. Phys.* **40**, 390 (1968).

<sup>2</sup> H. Primakoff and F. T. Porter, *Phys. Rev.* **89**, 930 (1953).

<sup>3</sup> The presence of  $L, M, \dots$ , electrons is ignored throughout the calculation.

<sup>4</sup> J. A. Miskel and M. L. Perlman, *Phys. Rev.* **94**, 1683 (1954).

<sup>5</sup> M. Langevin, *Compt. Rend.* **245**, 664 (1957); *J. Phys. Radium* **19**, 34 (1958).

<sup>6</sup> H. Daniel, G. Schupp, and E. N. Jensen, *Phys. Rev.* **117**, 823 (1960).

<sup>7</sup> J. G. Pengra and B. Crasemann, *Phys. Rev.* **131**, 2642 (1963).

<sup>8</sup> R. L. Intemann and F. Pollock, *Phys. Rev.* **157**, 41 (1967); hereafter referred to as I.

<sup>9</sup> P. C. Martin and R. J. Glauber, *Phys. Rev.* **109**, 1307 (1958).

<sup>10</sup> We shall only consider allowed transitions in this paper.

the shape of the ejected-electron spectrum. Furthermore, it is important to note that Primakoff and Porter could just as well have used an angular-momentum eigenstate of the unperturbed Hamiltonian rather than a scattering state to describe the ejected electron (even when screening and correlation effects are included). In this case their integration over the possible directions of the ejected electron is replaced by a summation over all possible final angular-momentum states which, owing to orthogonality, reduces to the single term with  $l=0$ .

To assess the effects of relativistic corrections, let us replace the nonrelativistic Coulomb eigenfunctions appearing in the overlap integral by their relativistic counterparts, i.e., by the corresponding solutions of the Dirac-Coulomb equation. As Stephas and Crasemann<sup>11</sup> have shown, this results in a substantial increase in the value of the absolute squared matrix element at all ejected-electron energies, even in the low-energy "non-relativistic" region. However, while the increase is significant at all energies, it is, as is to be expected, greatest at high energies. Since the experimental data are usually arbitrarily normalized to the theoretical curve in the high-energy region, the net effect of the relativistic corrections on the shape of the spectrum will be to bring about a relative lowering of the theoretical curve in the low-energy region (by roughly a factor of 2 to 3). This will indeed tend to bring theory and experiment into much better agreement.

Therefore, it is the purpose of the present paper to provide a more accurate theoretical treatment of the problem, one which includes all significant relativistic effects. At the same time, we wish to avoid using the eigenfunctions and Green's function of the relativistically exact Dirac-Coulomb Hamiltonian to describe the various electron states. The difficulties encountered in using these functions are well known and render an analytic solution to the problem impossible. In an attempt to get around such difficulties, Biedenharn and Swamy<sup>12</sup> have recently developed an approximately relativistic "symmetric Hamiltonian." As these authors have shown, the eigenfunctions of the symmetric Hamiltonian differ from the exact Dirac-Coulomb eigenfunctions by terms of order  $(Z\alpha)^2$  and therefore provide a basis for calculating the spectral intensity distribution of the ejected electrons to a relative accuracy of order  $(Z\alpha)^2$ . As we shall see, this approximation is sufficient to include all important relativistic effects. The great advantage in using the solutions of the symmetric Hamiltonian lies in the fact that these functions are no more difficult to work with than the solutions of the nonrelativistic Coulomb Hamiltonian.

In Sec. II we discuss the eigenfunctions and Green's functions of the symmetric Hamiltonian. Section III is devoted to the reduction of the transition matrix

element brought about by the use of the approximate solutions of Sec. II and the neglect of retardation effects. In Sec. IV the ejected-electron momentum spectrum is calculated in detail. In Sec. V the results of the theory are presented and comparison is made with both previous theoretical results and recent experimental observations.

## II. EIGENFUNCTIONS AND GREEN'S FUNCTIONS OF THE SYMMETRIC HAMILTONIAN

The symmetric Hamiltonian is a Dirac Hamiltonian which approximates the exact Dirac-Coulomb Hamiltonian to within an error of order  $(Z\alpha)^2/\kappa$ . We shall not attempt to present the actual motivation which led Biedenharn and Swamy to introduce the symmetric Hamiltonian; the reader is referred to their original paper<sup>12</sup> for such a discussion. Instead, following Biedenharn and Swamy, we shall simply define the symmetric Hamiltonian  $H_s$  from the "non-Hermitian Hamiltonian"  $\tilde{H}$  defined by<sup>13</sup>

$$\tilde{H} = S_1^2 H_P \equiv \{ \exp[ -\boldsymbol{\gamma} \cdot \hat{\boldsymbol{r}} \sinh^{-1}(a/K) ] \} (\boldsymbol{\alpha} \cdot \mathbf{P} + \beta), \quad (1)$$

where  $K$  is Dirac's operator. The Hermitian symmetric Hamiltonian is then defined by

$$H_s \equiv S_1^{-1} \tilde{H} S_1 = S_1 H_P S_1. \quad (2)$$

Biedenharn and Swamy<sup>12</sup> have already studied the discrete part of the spectrum of  $H_s$  and have shown that the energy eigenvalues and normalized energy eigenfunctions are, respectively,

$$E_n = (1 + a^2/n^2)^{-1/2}, \quad \Psi_{n,\kappa,\mu} = S_1^{-1} \tilde{\Psi}_{n,\kappa,\mu}, \quad (3)$$

where  $\tilde{\Psi}_{n,\kappa,\mu}$  is the eigenfunction of  $\tilde{H}$  corresponding to the same eigenvalue and is given by

$$\tilde{\Psi}_{n,\kappa,\mu} = \left( \frac{1}{2} E_n \right)^{1/2} \begin{pmatrix} -[1 + E_n(1 + a^2/\kappa^2)^{1/2}]^{1/2} F_{n,l(\kappa)}(\boldsymbol{r}) \phi_{\kappa}^{\mu} \\ \frac{a E_n [(n^2/\kappa^2 - 1)^{1/2} | F_{n,l(-\kappa)}(\boldsymbol{r}) |]}{n [1 + E_n(1 + a^2/\kappa^2)^{1/2}]^{1/2}} \phi_{-\kappa}^{\mu} \end{pmatrix} \quad (4)$$

The two-component spinors  $\phi_{\kappa}^{\mu}$  are the usual spin-angular functions of the Dirac theory,

$$\phi_{\kappa}^{\mu} = \sum_{m=\pm 1/2} C(l(\kappa), \frac{1}{2}, j; \mu - m, m, \mu) Y_{l(\kappa), m}^{\mu - m} \chi_{1/2}^m, \quad (5)$$

and satisfy

$$J^2 \phi_{\kappa}^{\mu} = j(j+1) \phi_{\kappa}^{\mu}, \quad (6)$$

$$J_z \phi_{\kappa}^{\mu} = \mu \phi_{\kappa}^{\mu}, \quad (7)$$

$$(\boldsymbol{\sigma} \cdot \mathbf{L} + 1) \phi_{\kappa}^{\mu} = -\kappa \phi_{\kappa}^{\mu}, \quad (8)$$

$$\boldsymbol{\sigma} \cdot \hat{\boldsymbol{r}} \phi_{\kappa}^{\mu} = i S(-\kappa) \phi_{-\kappa}^{\mu}, \quad (9)$$

<sup>11</sup> P. Stephas and B. Crasemann, Phys. Rev. **164**, 1509 (1967).

<sup>12</sup> L. C. Biedenharn and N. V. V. J. Swamy, Phys. Rev. **133**, B1353 (1964).

<sup>13</sup> As in I, we employ units in which  $m=c=\hbar=1$  and  $e^2=\alpha=1/137$ . The Dirac matrices are defined as  $\boldsymbol{\gamma} = -i\boldsymbol{\beta}\boldsymbol{\alpha}$  and  $\boldsymbol{\gamma}_4 = \beta$ ;  $\boldsymbol{\gamma}_5 = \boldsymbol{\gamma}_1\boldsymbol{\gamma}_2\boldsymbol{\gamma}_3\boldsymbol{\gamma}_4$  and  $\hat{\boldsymbol{\phi}} = \boldsymbol{\phi}\dagger\boldsymbol{\gamma}_4$ .

where  $S(\kappa)$  denotes the sign of  $\kappa$ . As in the nonrelativistic theory, the energy levels depend only on the principal quantum number  $n=1, 2, 3, \dots$ . As usual,  $l$  and  $j$  are related to  $\kappa$  by  $j=|\kappa|-\frac{1}{2}$ ;  $l(\kappa)=\kappa$  for  $\kappa>0$  and  $l(\kappa)=-\kappa-1$  for  $\kappa<0$ . The quantization condition restricts  $\kappa$  to the range  $-n\leq\kappa\leq n-1$ . Finally, in terms of the confluent hypergeometric function, the radial functions are given by

$$F_{n,l(\kappa)}(r) = Ce^{-k_n r} (2k_n r)^l F(-n+l+1, 2l+2, 2k_n r), \quad (10)$$

where  $k_n = aE_n/n$  and  $C$  is chosen so that

$$\int_0^\infty |F_{nl}|^2 r^2 dr = 1.$$

The method used by Biedenharn and Swamy to determine the bound states may also be used to determine the eigenfunctions of the continuous part of the spectrum of  $H_s$ . The analysis is similar and leads to the following results for the associated  $\Psi$ 's:

$$\tilde{\Psi}_{\kappa,\mu}(Pr) = N_\kappa \begin{pmatrix} -[1+W(1+a^2/\kappa^2)^{1/2}]F_{l(\kappa)}(Pr)\phi_{\kappa^\mu} \\ P|(1+a^2W^2/P^2\kappa^2)^{1/2}|F_{l(-\kappa)}(Pr)\phi_{-\kappa^\mu} \end{pmatrix} \quad (11)$$

where  $W$  is the total energy,  $P=(W^2-1)^{1/2}$ , and the radial functions are now given by

$$F_{l(\kappa)}(Pr) = \left(\frac{2}{\pi}\right)^{1/2} P e^{\pi a W/2P} \frac{|\Gamma(l+1-iaW/P)|}{(2l+1)!} \\ \times (2Pr)^l e^{-iPr} F(iaW/P+l+1, 2l+2, 2iPr). \quad (12)$$

With the continuum eigenfunctions normalized to the "P scale" [i.e., by the condition  $(\Psi_{\kappa,\mu}(Pr), \Psi_{\kappa,\mu}(P'r)) = \delta(P-P')$ ], the normalization constant is

$$N_\kappa = \{2[1+W(1+a^2/\kappa^2)^{1/2}] \\ \times [W(1+a^2/\kappa^2) + a(W^2(1+a^2/\kappa^2) - 1)^{1/2}/|\kappa|]\}^{-1/2}. \quad (13)$$

Now, let us consider the Green's function  $G_E^s(\mathbf{r}, \mathbf{r}')$  associated with the eigenvalue problem for  $H_s$ . It satisfies the equation

$$[H_s(\mathbf{r}) - E]G_E^s(\mathbf{r}, \mathbf{r}') = -\gamma_4\delta(\mathbf{r} - \mathbf{r}') \quad (14)$$

and its adjoint

$$G_E^s(\mathbf{r}, \mathbf{r}')\gamma_4[H_s(\mathbf{r}') - E] = -\delta(\mathbf{r} - \mathbf{r}'). \quad (15)$$

Like the eigenfunctions of  $H_s$ , the Green's function  $G_E^s(\mathbf{r}, \mathbf{r}')$  is most easily found by applying the appropriate projection operator to the corresponding Green's function  $g_E(\mathbf{r}, \mathbf{r}')$  of the second-order equation obtained by iterating either (14) or (15). To obtain this equation, we first rewrite the adjoint equation, with the aid of (1) and (2), as

$$S_1 G_E^s(\mathbf{r}, \mathbf{r}') S_1^{-1} (i\boldsymbol{\gamma} \cdot \mathbf{P}' + 1 - E\gamma_4 S_1^{-2}) \\ = -\delta(\mathbf{r} - \mathbf{r}'), \quad (16)$$

where we have made use of the fact that  $S_1\gamma_4 S_1 = \gamma_4$ . If we now iterate this equation by multiplying through from the right with  $i\boldsymbol{\gamma} \cdot \mathbf{P}' - 1 - E\gamma_4 S_1^{-2}$  and make use of the anticommutation relation

$$\{i\boldsymbol{\gamma} \cdot \mathbf{P}, \gamma_4 S_1^{-2}\}_+ = -2a/r, \quad (17)$$

we obtain the desired second-order equation

$$[\nabla^2 + (E^2 - 1) + 2aE/r']g_E(\mathbf{r}, \mathbf{r}') = -\delta(\mathbf{r} - \mathbf{r}'). \quad (18)$$

The Green's function  $S_1 G_E^s S_1^{-1}$ , which satisfies the first-order equation (16), is obtained from the second-order Green's function  $g_E$  by the application of the projection operator  $i\boldsymbol{\gamma} \cdot \mathbf{P}' - 1 - E\gamma_4 S_1^{-2}$ . From this we finally obtain for  $G_E^s$ ,

$$G_E^s(\mathbf{r}, \mathbf{r}') = S_1^{-1} [(i\boldsymbol{\gamma} \cdot \mathbf{P}' - 1 - E\gamma_4 S_1^{-2})g_E(\mathbf{r}, \mathbf{r}')] S_1. \quad (19)$$

For allowed transitions, the Green's function which appears in the matrix element for electron ejection has the particular form  $G_E^s(0, \mathbf{r})$  and is seen to satisfy a reduced form of (19):

$$G_E^s(0, \mathbf{r}) = [\boldsymbol{\gamma} \cdot \hat{\mathbf{r}}(\partial/\partial r) - 1 - \gamma_4 E]g_E(0, \mathbf{r}). \quad (20)$$

In obtaining (20) we have made use of the fact that  $g_E(0, \mathbf{r})$  is a spherically symmetric function. This is clear since it satisfies

$$[\nabla^2 + (E^2 - 1) + 2aE/r]g_E(0, \mathbf{r}) = -\delta(\mathbf{r}). \quad (21)$$

For  $K$ -capture transitions of interest (those for which there is no competing positron emission),  $|E| < 1$  and, as has already been mentioned in I, the Green's function does not represent a freely propagating wave, but rather is a function which decreases rapidly away from the nucleus. The solution of (21) which satisfies this boundary condition has already been obtained by Glauber and Martin<sup>14</sup> and may, for our purposes, be written

$$g_E(0, \mathbf{r}) = \frac{\mu}{2\pi} e^{-\mu r} \int_0^\infty ds e^{-2\mu r s} s^{-\eta} (1+s)^\eta, \quad (22)$$

with  $\mu = (1 - E^2)^{1/2}$  and  $\eta = aE/\mu$ . The Green's function  $G_E^s(0, \mathbf{r})$  is now completely determined by (20) and (22).

The eigenfunctions and Green's function described in this section differ from the corresponding Dirac-Coulomb functions by terms of order  $(Z\alpha)^2/|\kappa|$ . They therefore provide a basis for performing Coulomb field calculations in which relativistic effects are included to first order in  $(Z\alpha)$  beyond the nonrelativistic limit. For many applications, this is sufficient to include the major effects of relativity. At the same time, the mathematical structure of these functions is such as to make calculations employing them no more difficult than those employing nonrelativistic Coulomb functions. This is in sharp contrast to the situation in which

<sup>14</sup> R. J. Glauber and P. C. Martin, Phys. Rev. **104**, 158 (1956).

similar calculations are carried out using the exact Dirac-Coulomb functions.

### III. MATRIX ELEMENT FOR $K$ -ELECTRON EJECTION

The total matrix element for  $K$ -electron ejection has been derived in I. In that paper the electronic motions were described nonrelativistically, in which case it was expected and, indeed, demonstrated that retardation effects do not contribute to the initial-state electron-electron interaction. Since the distances involved are small, we expect that, even as a relativistic correction, these retardation effects will be quite small when compared to the relativistic spin corrections. We shall therefore again neglect such retardation effects in the present treatment. Under these circumstances, the total matrix element for  $K$ -electron ejection, for allowed  $K$ -capture transitions, is again given by Eq. (17) of I,<sup>15</sup>

$$M = -\alpha G[1 - P_{12}]\bar{\phi}'(0) \mathcal{B} \int d\mathbf{r}_1 g_E(0, \mathbf{r}_1) \gamma_4 \phi_1(\mathbf{r}_1) \times \int d\mathbf{r}_2 \phi_f^\dagger(\mathbf{r}_2) \phi_2(\mathbf{r}_2) (r_2^{-1} - r_{12}^{-1}). \quad (23)$$

To describe the electron states, we shall use the approximate relativistic wave functions and Green's function discussed in Sec. II. The matrix element may then be expressed in terms of the second-order Green's function  $g_E(0, \mathbf{r}_1)$  by substituting into it the expression (20) for  $G_E^s(0, \mathbf{r}_1)$ . After integrating over  $\mathbf{r}_1$ , by parts, we obtain

$$M = -\alpha G[1 - P_{12}]\bar{\phi}'(0) \mathcal{B} \times \int d\mathbf{r}_1 g_E(0, \mathbf{r}_1) \left( -\boldsymbol{\gamma} \cdot \hat{\mathbf{r}} \frac{\partial}{\partial r} - 1 - E\gamma_4 \right) \times \gamma_4 \phi_1(\mathbf{r}_1) \int d\mathbf{r}_2 \phi_f^\dagger(\mathbf{r}_2) \phi_2(\mathbf{r}_2) (r_2^{-1} - r_{12}^{-1}). \quad (24)$$

In order to proceed further, let us introduce the transformed wave function  $\bar{\phi}_1 = S_1 \phi_1$ . From (4) it is clear that, for a  $K$  electron,  $\bar{\phi}_1$  reduces to a spherically symmetric spinor whose lower two components vanish. Under these circumstances, the equation satisfied by  $\bar{\phi}_1$  is

$$[\boldsymbol{\gamma} \cdot \hat{\mathbf{r}} (\partial/\partial r) + 1 - E\gamma_4 S_1^{-2}] \bar{\phi}_1 = 0, \quad (25)$$

as readily follows from (1) and (2). Using these results, we find that (24) reduces to

$$M = -\alpha G[1 - P_{12}]\bar{\phi}'(0) \mathcal{B} \times \int d\mathbf{r}_2 \phi_f^\dagger(\mathbf{r}_2) \phi_2(\mathbf{r}_2) \int d\mathbf{r}_1 g_E(0, \mathbf{r}_1) \times \{2(r_{12}^{-1} - r_2^{-1}) + \boldsymbol{\gamma} \cdot \hat{\mathbf{r}}_1 [(\partial/\partial r_1) r_{12}^{-1}]\} S_1 \bar{\phi}_1(\mathbf{r}_1). \quad (26)$$

<sup>15</sup> The factor  $\gamma_4$  was set equal to 1 there, since we were using a nonrelativistic approximation for the electrons. Throughout this paper, we use the same basic notation as in I.

Since both  $g_E(0, \mathbf{r}_1)$  and  $\bar{\phi}_1(\mathbf{r}_1)$  are spherically symmetric functions, the integration over the angles of  $\mathbf{r}_1$  may conveniently be carried out at this time. To do so, we first rewrite  $S_1$  in the form

$$S_1 = A_\kappa - B_\kappa \boldsymbol{\gamma} \cdot \hat{\mathbf{r}}_1, \quad (27)$$

with

$$A_\kappa = [(1 + a^2/\kappa^2)^{1/2} + 1]^{1/2}/\sqrt{2}, \\ B_\kappa = [(1 + a^2/\kappa^2)^{1/2} - 1]^{1/2}/\sqrt{2}, \quad (28)$$

which follows from the definition (1). If we now substitute (27) for  $S_1$  (noting that  $\kappa = -1$  for the state  $\bar{\phi}_1$ ) and, for  $1/r_{12}$ , the integral representation

$$r_{12}^{-1} = \lim_{\epsilon \rightarrow 0} \frac{1}{2\pi^2} \int_{-\infty}^{\infty} \frac{d\mathbf{k} \exp[i\mathbf{k} \cdot (\mathbf{r}_1 - \mathbf{r}_2)]}{k^2 + \epsilon^2} \quad (29)$$

into (26), and carry out first the  $\mathbf{r}_1$  angular integration and then the integration over the angles of  $\mathbf{k}$ , we obtain for the transition matrix element the final form

$$M = -4\alpha G[1 - P_{12}]\bar{\phi}'(0) \mathcal{B} \int_{-\infty}^{\infty} \frac{k^2 dk}{k^2 + \epsilon^2} \int_0^\infty r^2 dr g_E(0, r) \times \{ [2A_1(j_0(kr) - 1) - B_1 k j_1(kr)] \mathcal{g}_0 + [A_1 k j_0(kr) - 2B_1 j_1(kr)] \mathcal{g}_1 \} \bar{\phi}_1(\mathbf{r}_1), \quad (30)$$

where

$$\mathcal{g}_0 = \int d\mathbf{r} \phi_f^\dagger(\mathbf{r}) \phi_2(\mathbf{r}) j_0(kr), \quad (31)$$

$$\mathcal{g}_1 = \int d\mathbf{r} \phi_f^\dagger(\mathbf{r}) \phi_2(\mathbf{r}) j_1(kr) \boldsymbol{\gamma} \cdot \hat{\mathbf{r}}. \quad (32)$$

These last integrals may be further simplified by introducing the transformed wave functions  $\bar{\phi}_2$  and  $\bar{\phi}_f$ , as before, and expression (27) for  $S_1$

$$\mathcal{g}_0 = \int d\mathbf{r} \bar{\phi}_f^\dagger (C_\kappa + D_\kappa \boldsymbol{\gamma} \cdot \hat{\mathbf{r}}) \bar{\phi}_2 j_0(kr), \quad (33)$$

$$\mathcal{g}_1 = \int d\mathbf{r} \bar{\phi}_f^\dagger (C_\kappa + D_\kappa \boldsymbol{\gamma} \cdot \hat{\mathbf{r}}) \bar{\phi}_2 j_1(kr) \boldsymbol{\gamma} \cdot \hat{\mathbf{r}}, \quad (34)$$

with  $C_\kappa = A_\kappa A_1 + B_\kappa B_1$  and  $D_\kappa = A_1 B_\kappa + B_1 A_\kappa$ .

### IV. EJECTED-ELECTRON TRANSITION RATE

We begin our evaluation of the relative differential transition rate for  $K$ -electron ejection with the evaluation of the integrals  $\mathcal{g}_0$  and  $\mathcal{g}_1$ , for which purpose we must introduce detailed forms for the electron states which appear. For  $\bar{\phi}_2$ , we choose a  $K$ -electron wave function, while, for the ejected electron, we choose a continuum angular-momentum eigenfunction  $\Psi_{\kappa\mu}(Pr)$  of the symmetric Hamiltonian. This is appropriate, since we are not concerned with the direction in which the electron is ejected but only with its energy probability distribution, which may be obtained by summing over all possible final angular-momentum states of the ejected electron. As we shall see, in our approximation

very few such states actually contribute to the transition rate.

The appropriate wave functions are obtained from (4) and (11) and, after substitution into (33) and (34), lead to the result

$$g_n = S_n(k) g_n, \quad n=0, 1 \quad (35)$$

with

$$S_n(k) = E_1^2 (a^3/\pi)^{1/2} N_\kappa \{ C_\kappa [1 + W(1 + a^2/\kappa^2)^{1/2}] R_{n, l(\kappa)} - PS(\kappa) D_\kappa (1 + a^2 W^2/P^2 \kappa^2)^{1/2} R_{n, l(-\kappa)} \}, \quad (36)$$

in which the radial integrals are defined by

$$R_{n, l(\kappa)} = \int_0^\infty r^2 dr F_{l(\kappa)}^*(Pr) e^{-aEr} j_n(kr). \quad (37)$$

The angular integrals  $g_n$  are given by

$$g_n = \int d\Omega \phi_{\mu_f}^{\mu_f \dagger} \chi_2 \Theta_n, \quad (38)$$

with  $\Theta_0 = 1$  and  $\Theta_1 = \gamma \cdot \hat{r}$ .

In writing (38), we have suppressed the indices  $\kappa$  and  $\mu_f$  upon which the  $g_n$  depend. With the use of (5), the angular integrals are easily evaluated, with the result

$$g_0 = (4\pi)^{1/2} \delta_{\mu_f, \mu_2} \delta_{\kappa, -1}, \quad (39)$$

$$g_1 = -i(4\pi)^{1/2} C(1, \frac{1}{2}, j; 0, \mu_2, \mu_2) (|\gamma|/\sqrt{3}) \delta_{\mu_f, \mu_2} \delta_{1, l(\kappa)}. \quad (40)$$

From these results we see that the only final states available to the ejected electron (in our approximation) are those for which  $\kappa = -1, +1, -2$ , and we must therefore evaluate our transition matrix element only for these three types of states. Using the results (35), (39), and (40), we then obtain, for the transition matrix element (30),

$$M = -8\alpha G E_1^2 a^{3/2} [1 - P_{12}] \bar{\phi}^{\nu}(0) \mathcal{B} \delta_{\mu_f, \mu_2} \times \{ \mathcal{F}_\kappa \delta_{\kappa, -1} - iC(1, \frac{1}{2}, j; 0, \mu_2, \mu_2) (|\gamma|/\sqrt{3}) \mathcal{G}_\kappa \delta_{1, l(\kappa)} \} \chi_1^{(+)}, \quad (41)$$

with

$$\mathcal{F}_\kappa \equiv \int_{-\infty}^{\infty} \frac{k^2 dk}{k^2 + \epsilon^2} \int_0^\infty r^2 dr g_E(0, r) e^{-aEr} S_0 \times [2A_1 \{ j_0(kr) - 1 \} - B_1 k j_1(kr)], \quad (42)$$

$$\mathcal{G}_\kappa \equiv \int_{-\infty}^{\infty} \frac{k^2 dk}{k^2 + \epsilon^2} \int_0^\infty r^2 dr g_E(0, r) e^{-aEr} S_1(k) \times [A_1 k j_0(kr) - 2B_1 j_1(kr)], \quad (43)$$

and with

$$\chi_1^{(+)} = \begin{pmatrix} \chi_1 \\ 0 \end{pmatrix}.$$

To determine the transition rate, we must sum the squared absolute value of  $M$  over the spin states of the

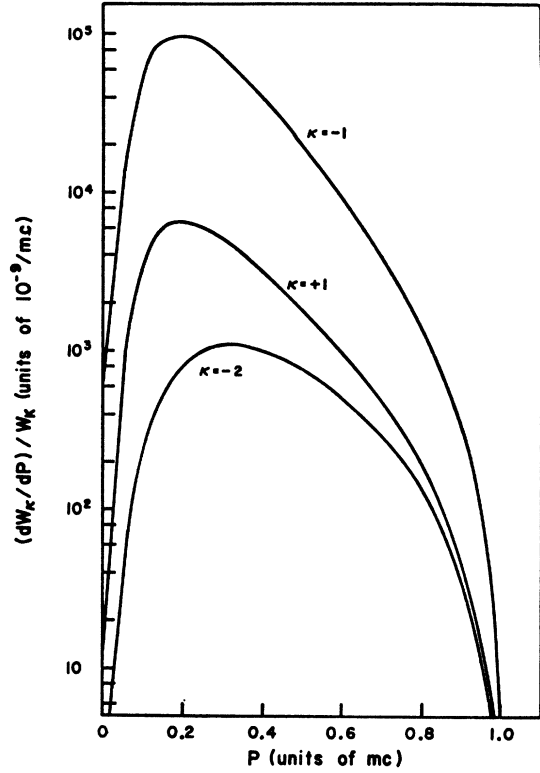


FIG. 1. Partial rate curves contributing to the predicted momentum spectrum of K electrons ejected during K capture by  $Fe^{56}$ . The theoretical end point is at  $P = 1.015$ .

two emitted leptons and the two initial K electrons. The calculation is easily carried out using standard techniques and, for unaligned nuclei, leads to the results

$$\sum_{\mu_f, \mu_2, \mu_1, \mu_2} |M_{-1}|^2 = (2^5 \alpha^2 / \pi^3) G^2 E_1^4 a^3 B \cdot B^* |\mathcal{F}_{-1}|^2, \quad (44)$$

$$\sum_{\mu_f, \mu_2, \mu_1, \mu_2} |M_\kappa|^2 = (2^5 \alpha^2 / \pi^3) G^2 E_1^4 a^3 B \cdot B^* \times |C(1, \frac{1}{2}, j; 0, \mu_2, \mu_2)|^2 |\mathcal{G}_\kappa|^2, \quad \kappa = +1, -2 \quad (45)$$

for those final states contributing to the process. The corresponding differential transition rate may then be obtained from Eq. (22) of I

$$dw_\kappa/dP = 8\pi^3 P^2 (1+Q-W)^2 \sum |M_\kappa|^2, \quad (46)$$

where  $Q$  is the energy released in the decay process. In order to obtain the relative rate for K-electron ejection, we must also know the transition rate for allowed K capture. In the approximation defined by the eigenstates of the symmetric Hamiltonian, this is easily found to be

$$w_K = (G^2 a^3 / \pi^2) E_1^3 (1+Q-E_1)^2 B \cdot B^*. \quad (47)$$

Combining (44)-(47), we obtain for the relative transition rate for the ejection of a K electron into the

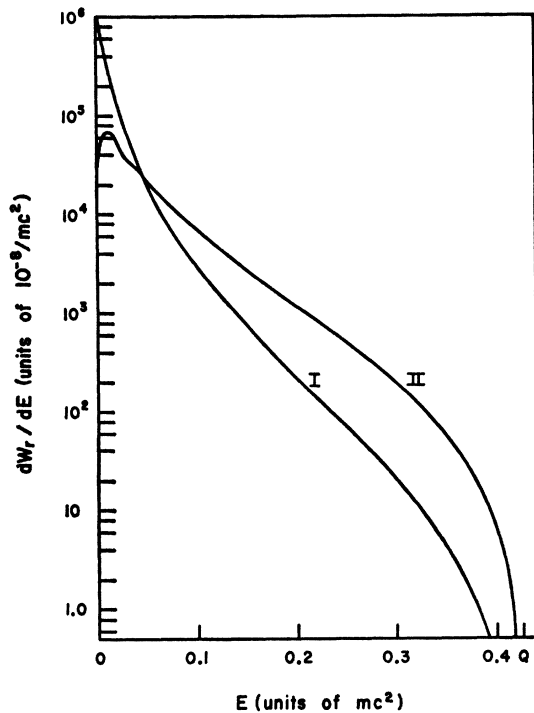


FIG. 2. Theoretical energy spectrum of  $K$  electrons ejected during  $K$  capture by  $\text{Fe}^{56}$ . Curve I represents the result of the nonrelativistic theory of I, while curve II represents the result of the present theory. The theoretical end point is at  $Q=0.425$ .

momentum range  $dP$

$$\begin{aligned} dw_{\kappa}/dP &\equiv w_{\kappa}^{-1} \sum_{\kappa=-1,+1,-2} (dw_{\kappa}/dP) \\ &= 2^8 \alpha^2 \pi^2 E_1 P^2 \left( \frac{1+Q-W}{1+Q-E_1} \right)^2 \\ &\quad \times [ |\mathcal{F}_{-1}|^2 + \frac{1}{3} | \mathcal{G}_{+1} |^2 + \frac{2}{3} | \mathcal{G}_{-2} |^2 ]. \quad (48) \end{aligned}$$

The evaluation of the remaining integrals,  $\mathcal{F}_{-1}$ ,  $\mathcal{G}_{+1}$ , and  $\mathcal{G}_{-2}$ , is carried out in the Appendix and leads to the final results given by (A7), (A12), (A13), and supporting equations. Since the final forms are rather complicated, we shall not repeat them here. These results, together with (48), completely determine the ejected-electron differential transition rate per  $K$ -capture event.

Figure 1 illustrates the form of the partial rate curve  $(dw_{\kappa}/dP)/w_{\kappa}$  for each of the three terms ( $\kappa=-1, +1, -2$ ) which contribute to the transition rate for the case of  $\text{Fe}^{56}$ , which has a maximum ejected-electron momentum of 519 keV/c. The dominant term, as expected, is the one for which the electron is ejected in an  $s_{1/2}$  state, while the rate for ejection in a  $p_{1/2}$  state never represents more than about a 10% correction. Furthermore, at low momenta ( $P \lesssim 0.2 \text{ mc}$ ) the rate

for ejection in a  $p_{3/2}$  state is only about 10% of that for ejection in a  $p_{1/2}$  state; however, at higher momenta these two rates do become comparable.

As a result, the total differential transition rate is largely determined by the  $\kappa=-1$  contribution to it. Indeed, since the shapes of all three curves are roughly the same, we expect the shape of the total rate curve to be essentially the same as that of the  $\kappa=-1$  curve. This is borne out by a plot of the total rate curve which, on the scale used in Fig. 1, yields a curve which almost completely overlaps the  $\kappa=-1$  curve. For this reason, we have not included it in the figure.

Finally, it should be pointed out that a comparison of any experimental data with the theoretical spectrum is most easily accomplished by employing a construction analogous to the Fermi plot used in the analysis of  $\beta$  spectra. The idea was first suggested by Primakoff and Porter<sup>2</sup> in connection with their theory and, in the case of the present theory, consists of plotting

$$\{N(E)/PW[|\mathcal{F}_{-1}|^2 + \frac{1}{3} | \mathcal{G}_{+1} |^2 + \frac{2}{3} | \mathcal{G}_{-2} |^2]\}^{1/2}$$

versus  $E$ , in which  $N(E)$  is the number of electrons ejected with kinetic energy  $E$ . According to (48), such a plot should yield a straight line which intercepts the  $E$  axis at  $E=Q$ .

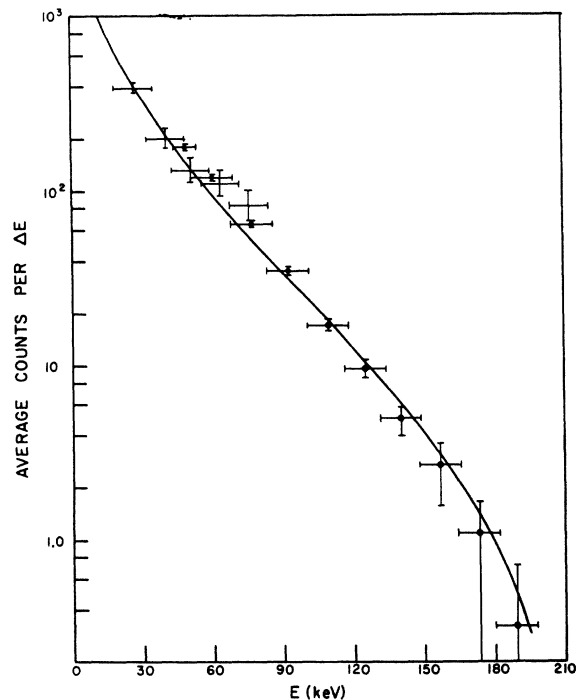


FIG. 3. Spectrum of electrons ejected during the electron-capture decay of  $\text{Fe}^{56}$  [taken from Pengra and Crasemann (Ref. 7)]. The closed circles represent measurements with a solid-state detector; the remaining points were obtained with a proportional counter. The solid curve represents the theoretical spectrum predicted by the present theory.

## V. RESULTS AND CONCLUSIONS

The energy spectrum of  $K$  electrons ejected during  $K$  capture is obtained by transforming (48) to the energy scale and is illustrated, for the case of  $\text{Fe}^{55}$ , by curve II in Fig. 2. For comparison, we have also plotted the spectrum predicted by the nonrelativistic theory of I.<sup>16</sup> This spectrum is represented by curve I in Fig. 2. The present theory predicts the ejection of substantially more electrons at all but the very lowest energies (the increase increasing with energy) and, more importantly for current experiments, it predicts a spectrum whose shape is significantly different from that predicted by the nonrelativistic theory.

The most extensive experimental study on the spectral distribution of electrons ejected during electron capture has been that of Pengra and Crasemann.<sup>7</sup> These investigators have measured the ejected-electron spectrum arising from the decay of  $\text{Fe}^{55}$  over a wide range of energies. The results of their measurements are reproduced in Fig. 3. For comparison, we have also plotted the theoretical energy spectrum predicted by the present theory. The theoretical curve has been normalized to the experimental data in the high-energy region by employing the construction described at the end of Sec. IV.

It is clear from Fig. 3 that there is complete agreement between the spectrum measured by Pengra and Crasemann and the spectrum predicted by the present theory. We have also examined the earlier and less extensive data of Daniel, Schupp, and Jensen<sup>6</sup> on  $\text{Cs}^{131}$ . Here too we have found good agreement between the measured values and the predictions of the present theory.

The importance of relativistic effects in the electron ejection process is now clear. Although retardation effects are of no consequence, relativistic spin effects play a most important role. In the nonrelativistic theory the electron can only be ejected in  $s_{1/2}$  states. Relativistic effects allow for ejection in  $p_{1/2}$  and  $p_{3/2}$  states as well, although, as we have seen, it is the relativistic correction to the  $s_{1/2}$  state amplitude which accounts for almost all of the changes in the theoretical spectrum.

## ACKNOWLEDGMENTS

The author wishes to express his appreciation to Dr. A. Auerbach and Dr. V. Highland for their guidance and assistance with the computing and to the Temple University Computer Activity for the allocation of computer time. He would also like to thank Dr. B. Steinberg for his help in the preparation of the figures.

## APPENDIX

In this Appendix we shall evaluate the integrals  $\mathfrak{F}_{-1}$ ,  $\mathfrak{G}_{+1}$ , and  $\mathfrak{G}_{-2}$ , which appear in our final expression for

<sup>16</sup> The spectrum predicted by the theory of I is virtually identical to the one predicted by the Primakoff-Porter theory.

the transition rate. In order to outline the basic steps involved, let us consider first  $\mathfrak{F}_{-1}$ . With the introduction of the representation (22) for  $g_{\mathbf{E}}(0, \mathbf{r})$  into expression (42) for  $\mathfrak{F}_{-1}$ , the radial integration becomes elementary and yields the result

$$\mathfrak{F}_{-1} = \frac{\mu}{\pi} \int_0^\infty ds \left( \frac{1+s}{s} \right)^{\eta} \int_{-\infty}^{\infty} \frac{k^2 dk}{k^2 + \epsilon^2} \times S_0(k) \left( \frac{2A_1\sigma - B_1k^2}{(k^2 + \sigma^2)^2} - \frac{2A_1}{\sigma^3} \right), \quad (\text{A1})$$

where  $\sigma = \mu(1+2s) + aE_1$ , and where, from (36),  $S_0(k)$  is now

$$S_0(k) = E_1^2 (a^3/\pi)^{1/2} N_1 \{ C_1 [1 + W(1+a^2)^{1/2}] R_{0,0} + PD_1 (1+a^2W^2/P^2)^{1/2} R_{0,1} \}. \quad (\text{A2})$$

The radial integrals  $R_{0,i}$  are given by (37), with  $F_l(P\mathbf{r})$  given by (12). Introducing the standard integral representation for the confluent hypergeometric function,<sup>17</sup> we may carry out the radial integration in  $R_{0,i}$ , again by elementary methods, obtaining

$$R_{0,i} = \frac{i^i (l+1)!}{(2\pi)^{3/2}} P e^{\sigma a W/2P} (2P)^i \times \frac{|\Gamma(l+1+iaW/P)|}{\Gamma(l+1+iaW/P)} \Gamma(-l+iaW/P) \times \oint_C dt (-t)^{l-iaW/P} (1-t)^{l+iaW/P} k^{-1} \times \left( \frac{1}{(k+i\lambda)^{l+2}} - \frac{(-1)^l}{(k-i\lambda)^{l+2}} \right), \quad (\text{A3})$$

with  $\lambda = aE_1 + iP(2l-1)$ . The contour of integration  $C$  encircles the branch cut extending from 0 to 1 along the real axis in the positive sense and must satisfy the requirement  $\text{Im}l < aE_1/2P$  to ensure convergence of the radial integral.

To perform the  $k$  integration we observe, from the above results, that the integrand of the  $k$  integral falls off sufficiently rapidly for large values of  $k$  to allow us to close the  $k$ -integration contour at infinity. The use of residue theory then leads to the result

$$\mathfrak{F}_{-1} = \frac{\mu E_1^2}{(2\pi)^{3/2}} \left( \frac{a^3}{\pi} \right)^{1/2} N_1 \frac{e^{\sigma a W/2P}}{4P^2} \times \frac{|\Gamma(1+iaW/P)|}{\Gamma(1+iaW/P)} \Gamma(iaW/P) \int_0^\infty \frac{ds}{\sigma^2} \left( \frac{1+s}{s} \right)^{\eta} \times \{ C_1 [1 + W(1+a^2)^{1/2}] T_1 + iPD_1 T_2 \}, \quad (\text{A4})$$

<sup>17</sup> L. J. Slater, *Confluent Hypergeometric Functions* (Cambridge University Press, Cambridge, England, 1960), p. 40.

with

$$T_1 = \oint_C dt (-t)^{-i\alpha W/P} (1-t)^{i\alpha W/P} \left( \frac{4iPA_1}{\sigma(t-t_0)^2} + \frac{2A_1+B_1\sigma}{(t-t_0)^3} \right), \tag{A5}$$

$$T_2 = \oint_C dt (-t)^{1-i\alpha W/P} (1-t)^{1+i\alpha W/P} \times \left( \frac{8iPA_1}{\sigma(t-t_0)^3} + \frac{3(2A_1+B_1\sigma)}{(t-t_0)^4} \right). \tag{A6}$$

In writing the above results we have made use of the definitions of  $\sigma$  and  $\lambda$  and introduced

$$t_0 = [P + i(aE_1 + \sigma)]/2P.$$

The  $t$  integration may now be carried out in a similar manner. From the structure of the integrands in (A5) and (A6), we see that we may freely add to the contour  $C$  a circular contour at infinity and, again, evaluate the integrals by residue theory. The results of the integration, together with a change in the remaining integration variable  $s$  to  $x = s/(1+s)$  and a good deal of algebraic manipulation, finally allow us to write  $\mathfrak{F}_{-1}$ , in terms of certain fundamental integrals, as

$$\mathfrak{F}_{-1} = L_{-1} \left[ \Gamma I + \sum_{n=2}^5 \Gamma_n I_n \right], \tag{A7}$$

in which  $L_{-1}$  is determined from<sup>18</sup>

$$L_{\kappa} = \frac{2iaW\mu E_1^2}{\pi\Delta^3\Sigma^2} \left( \frac{1}{2} a^3 \right)^{1/2} e^{\sigma a W/2P} \kappa N_{\kappa} \Gamma(1 - |\kappa| + iaW/P), \tag{A8}$$

with  $\Delta = \mu + aE_1$  and  $\Sigma = P^2 + (2aE_1 + \mu)^2$ . The fundamental integrals which appear are defined by

$$I = \int_0^1 \frac{dx x^{-\nu} (1-x) (1-e^{-\nu})}{(1+\lambda x)^3}, \tag{A9}$$

$$I_n = \int_0^1 \frac{dx x^{-\nu} (1-x)^n e^{-\nu}}{(1+\lambda x)^{n-2} (1+\epsilon x + \delta x^2)^2}, \tag{A10}$$

in which

$$\begin{aligned} \lambda &= (\mu - aE_1)/\Delta, \\ \epsilon &= 2(\mu^2 - 4a^2E_1^2 - P^2)/\Sigma, \\ \delta &= [P^2 + (\mu - 2aE_1)^2]/\Sigma, \end{aligned}$$

and

$$y = (2aW/P) \tan^{-1} \left( \frac{P(1-x)}{(\mu + 2aE_1) + (\mu - 2aE_1)x} \right).$$

To simplify the writing of the coefficients appearing in (A7), we first introduce the following set of definitions:

with

$$\begin{aligned} \epsilon &= aE_1, & \bar{P} &= P/\epsilon, & \rho_1 &= 1 + \bar{P}^2, \\ \omega &= aW/\epsilon, & \bar{B}_{\kappa} &= B_{\kappa}/\epsilon, & \rho_2 &= C_1(1 + W/E_1)/\epsilon, \\ \beta_{\pm} &= 1 \pm \omega, & \bar{\Delta} &= \Delta/\epsilon, & \rho_3 &= \bar{P}^2 + \omega^2, \\ \gamma_{\pm} &= 3 \pm \omega, & \bar{\Sigma} &= \Sigma/\epsilon, & \rho_4 &= 2C_2(1 + W/E_2)/\epsilon, \end{aligned}$$

in terms of which the coefficients are given by

$$\Gamma = \bar{\Sigma}^2 [\bar{B}_1(\epsilon + a) + aA_1]/2\omega, \tag{A11a}$$

$$\Gamma_2 = \bar{\Delta}^3 [\bar{B}_1 \epsilon^2 \rho_2 - 2A_1 D_1], \tag{A11b}$$

$$\Gamma_3 = \bar{\Delta}^2 [\rho_2(4A_1 + \epsilon^2 \bar{B}_1 \beta_-) + \epsilon^2 \bar{B}_1 \rho_3 D_1 - 2A_1 D_1 \gamma_+], \tag{A11c}$$

$$\Gamma_4 = 2A_1 \bar{\Delta} [\rho_2 \gamma_- - D_1(\gamma_+ + \omega \beta_-)], \tag{A11d}$$

$$\Gamma_5 = 2A_1 \rho_1 [\rho_2 - D_1 \beta_+]. \tag{A11e}$$

The reduction of the two remaining integrals,  $\mathfrak{G}_{+1}$  and  $\mathfrak{G}_{-2}$ , may be carried out in a similar manner, with the final results

$$\mathfrak{G}_{+1} = L_{+1} \left[ \sum_{n=1}^5 \Lambda_n I_n + \Lambda_6 J_1 + \Lambda_7 J_2 \right], \tag{A12}$$

$$\mathfrak{G}_{-2} = L_{-2} \left[ \sum_{n=1}^5 R_n I_n + R_6 J_1 + R_7 J_2 \right], \tag{A13}$$

in which there appear the two additional fundamental integrals

$$J_n = \int_0^1 \frac{dx x^{-\nu} (1-x)^n (e^{-u} - e^{-v})}{(1+\lambda x)^{n+2}}, \quad n=1, 2 \tag{A14}$$

with  $u = (2aW/P) \tan^{-1}(P/aE_1)$ . Using our previous definitions, we find for the two sets of coefficients

$$\Lambda_1 = A_1 \bar{\Delta}^4 \rho_2 / \epsilon \rho_3^{1/2}, \tag{A15a}$$

$$\Lambda_2 = \bar{\Delta}^3 [A_1(2D_1 \rho_3 + \rho_2 \gamma_+) - 2\bar{B}_1 \rho_2] / \epsilon \rho_3^{1/2}, \tag{A15b}$$

$$\Lambda_3 = \bar{\Delta}^2 [A_1(D_1 \rho_3 \gamma_- + \rho_2 \gamma_+ + \omega \rho_2 \beta_-) - 2\bar{B}_1(2D_1 \rho_3 + \rho_2 \gamma_+)] / \epsilon \rho_3^{1/2}, \tag{A15c}$$

$$\Lambda_4 = \Delta [A_1 \rho_1 (\rho_2 \beta_+ + D_1 \rho_3) - 2\bar{B}_1(D_1 \rho_3 \gamma_- + \rho_2 \gamma_+ + \rho_2 \omega \beta_-)] / \epsilon \rho_3^{1/2}, \tag{A15d}$$

$$\Lambda_5 = -2\bar{B}_1 \rho_1 [\rho_2 \beta_+ + D_1 \rho_3] / \epsilon \rho_3^{1/2}, \tag{A15e}$$

$$\Lambda_6 = -A_1 \bar{\Sigma}^2 \epsilon \Lambda_5 / 4\bar{B}_1 \omega \rho_1, \tag{A15f}$$

$$\Lambda_7 = \bar{\Sigma}^2 \epsilon \Lambda_5 / 2\omega \rho_1 \bar{\Delta} \tag{A15g}$$

and

$$R_1 = A_1 \bar{\Delta}^4 [\rho_4 - 3D_2]/4P, \tag{A16a}$$

$$R_2 = \bar{\Delta}^3 [\rho_4(A_1 \gamma_+ - 2\bar{B}_1) - D_2(3A_1 \gamma_+ - A_1 \rho_3 - 6\bar{B}_1)]/4P, \tag{A16b}$$

<sup>18</sup> In writing  $L_{\kappa}$ , we have omitted the phase factor  $|\Gamma(|\kappa| + iaW/P)|/|\Gamma(|\kappa| + iaW/P)|$ , since only  $|L_{\kappa}|^2$  appears in the transition rate.

$$R_3 = \bar{\Delta}^2 [\rho_4 (A_1 \gamma_+ + A_1 \omega \beta_- - 2\bar{B}_1 \gamma_+) - D_2 \{ A_1 (3\rho_1 + 6\beta_+ - \omega\rho_3) - 2\bar{B}_1 (3\gamma_+ - \rho_3) \}] / 4P, \quad (\text{A16c})$$

$$R_4 = \bar{\Delta} [\rho_4 \{ A_1 \beta_+ \rho_1 - 2\bar{B}_1 (\gamma_+ + \omega\beta_-) \} - D_2 \{ A_1 \rho_1 (3\beta_+ + \rho_3 P^2) - 2\bar{B}_1 (3\rho_1 + 6\beta_+ - \omega\rho_3) \}] / 4P, \quad (\text{A16d})$$

$$R_5 = \bar{B}_1 [-\rho_4 \beta_+ \rho_1 + D_2 \rho_1 (3\beta_+ + \rho_3 P^2)] / 2P, \quad (\text{A16e})$$

$$R_6 = A_1 \bar{\Sigma}^2 [\rho_4 \beta_+ - D_2 (3\beta_+ + \rho_3)] / 8P\omega, \quad (\text{A16f})$$

$$R_7 = -2\bar{B}_1 R_6 / A_1 \bar{\Delta}. \quad (\text{A16g})$$

To complete the analysis we must evaluate the fundamental integrals (A9), (A10), and (A14). Although this cannot be done in closed form, rapidly converging series expansions are obtainable using the same method

as employed in I. We observe that all the fundamental integrals are of the form

$$F_n = \int_0^1 dx x^{-\eta} (1-x)^{\eta} f_n(x). \quad (\text{A17})$$

Detailed examination reveals that the  $f_n(x)$  are relatively slowly varying functions over the interval  $0 \leq x \leq 1$  for all cases. The structure of the integrand then suggests that, if  $f_n(x)$  is expanded in a Maclaurin series, the resulting series for  $F_n$  will converge quite rapidly. Performing such an expansion, we obtain

$$F_n = n! \sum_{k=0}^{\infty} \frac{f_n^{(k)}(0)}{k!(1+k-\eta)(2+k-\eta)\cdots(n+1+k-\eta)}, \quad (\text{A18})$$

from which the various fundamental integrals may then be evaluated.

## Triton Reactions near 2 MeV: Elastic Scattering

G. H. HERLING,\* L. COHEN, AND J. D. SILVERSTEIN†

Naval Research Laboratory, Washington, D. C. 20390

(Received 19 August 1968)

Tritons have been elastically scattered from a number of light nuclei, and the data have been analyzed in terms of the optical model. Geometries have been found which are applicable to  ${}^9\text{Be}$ ,  ${}^{10,11}\text{B}$ , and  ${}^{12}\text{C}$ , and to  ${}^{19}\text{F}$  and  ${}^{20}\text{Ne}$ . The real central well depths are approximately 140 MeV, and the spin-orbit well depth is greater than that expected from theoretical considerations. Ambiguities in the parameters are discussed.

### 1. INTRODUCTION

THERE has recently been much interest in the scattering and reactions induced by mass-three particles. Because of the success in describing the elastic scattering of deuterons and  $\alpha$  particles with the optical model, a similar analysis for the scattering of  ${}^3\text{H}$  appears plausible. Many optical-model analyses of  ${}^3\text{He}$  scattering have been performed,<sup>1</sup> but there have been relatively few analyses for tritons.<sup>2-8</sup> The present paper is concerned with an optical-model analysis of the elastic

scattering of tritons with bombarding energies near 2 MeV.

Although the triton energy is low, the scattering from the target nuclei  ${}^9\text{Be}$ ,  ${}^{10}\text{B}$ ,  ${}^{11}\text{B}$ ,  ${}^{12}\text{C}$ ,  ${}^{19}\text{F}$ , and  ${}^{20}\text{Ne}$  generally exhibits structure that is capable of yielding optical-model parameters which may be further tested by their employment in distorted-wave Born approximation (DWBA) calculations. In order to reduce the region of the parameter space searched, the results of other analyses have been used to obtain starting points for the calculations. Additional constraints on the acceptable solutions are supplied by the theoretical model, which suggests that the optical potential for a complex projectile should be the sum of the nucleon optical potentials for its constituents averaged over their internal wave function.<sup>9-12</sup>

In Secs. 2 and 3 the triton experiments and optical-model analysis are briefly considered. In Sec. 4 there

\* Present address: State University of New York, Stony Brook, N.Y. On leave from the Naval Research Laboratory.

† National Research Council, U.S. Naval Research Laboratory Postdoctoral Resident Research Associate.

<sup>1</sup> P. E. Hodgson, Institute of Physical and Chemical Research Cyclotron Progress Report Suppl. 1, 1968, p. 41 (unpublished).

<sup>2</sup> D. J. Pullen, J. R. Rook, and R. Middleton, Nucl. Phys. 51, 88 (1964).

<sup>3</sup> J. H. Bjeregaard, H. R. Blieden, O. Hansen, G. Sidenius, and G. R. Satchler, Phys. Rev. 136, B1348 (1964).

<sup>4</sup> J. R. Rook, Nucl. Phys. 61, 219 (1965).

<sup>5</sup> R. N. Glover and A. D. W. Jones, Phys. Letters 16, 69 (1965).

<sup>6</sup> R. N. Glover and A. D. W. Jones, Nucl. Phys. 81, 268 (1966).

<sup>7</sup> A. G. Blair and D. D. Armstrong, Phys. Rev. 151, 930 (1966).

<sup>8</sup> J. C. Hafele, E. R. Flynn, and A. G. Blair, Phys. Rev. 155, 1238 (1967).

<sup>9</sup> S. Watanabe, Nucl. Phys. 8, 484 (1958).

<sup>10</sup> J. L. Gammel, B. J. Hill, and R. M. Thaler, Helv. Phys. Acta Suppl. 6, 409 (1961).

<sup>11</sup> A. Y. Abul-Magd and M. El-Nadi, Progr. Theoret. Phys. (Kyoto) 35, 798 (1966).

<sup>12</sup> L. R. Veaser, D. D. Armstrong, and P. W. Keaton, Jr., Bull. Am. Phys. Soc. Ser. II, 13, 117 (1968).